

Rotation profiles of solar-like stars with magnetic fields

Wuming Yang¹ and Shaolan Bi^{2,3}

¹ Department of Physics and Chemistry, Henan Polytechnic University, Jiaozuo 454000, PR China. wuming.yang@hotmail.com

² Department of Astronomy, Beijing Normal University, Beijing 100875, China. bisl@bnu.edu.cn

³ National Astronomical Observatories/Yunnan Observatory, Chinese Academy of Sciences, Kunming 650011, China

Abstract The aim of this work is to investigate rotation profile of solar-like stars with magnetic fields. A diffusion coefficient of magnetic angular momentum transport is deduced. Rotating stellar models with different mass are computed under the effect of the coefficient. Then rotation profiles are obtained from the theoretical stellar models. The total angular momentum of solar model with only hydrodynamic instabilities is about 13 times larger than that of the Sun at the age of the Sun, and this model can not reproduce quasi-solid rotation in the radiative region. However, not only can the solar model with magnetic fields reproduce an almost uniform rotation in the radiative region, but its total angular momentum is consistent with helioseismic result at the level of 3σ at the age of the Sun. The rotation of solar-like stars with magnetic fields is almost uniform in the radiative region. But there is an obvious transition region of angular velocity between the convective core and the radiative region of models with $1.2 - 1.5 M_{\odot}$, where angular velocity has a sharp radial change, which is different from the rotation profile of the Sun and massive stars with magnetic fields. Moreover the changes of the angular velocity in the transition region increase with the increasing in the age and mass.

Key words: stars: evolution – stars: rotation – stars: magnetic fields

1 INTRODUCTION

Helioseismology has given us detailed internal information about the structure and rotation of the Sun: the Sun's rotation is slow in the core and is almost uniform in the radiative region, but the angular velocity has a latitudinal gradient in the convective zone (Gough et al. 1996; Schou et al. 1998; Chaplin et al. 1999). Although the data of inversion of solar-like stars are limited, it has been revealed

* E-mail: yangwuming@ynao.ac.cn

that the localized information of stellar interior can be given by asteroseismology (Gough & Kosovichev 1993; Gough 1998; Roxburgh et al. 1998; Berthomieu et al. 2001; Basu et al. 2002; Basu 2003). Furthermore, it has been shown that localized information on the internal rotation profile of a solar-like star can be obtained from the frequencies of oscillations (Gough & Kosovichev 1993; Gough 1998; Goupil et al. 1996; Lochard et al. 2004, 2005). The information on the internal rotation of β Cepheid has already been provided by asteroseismology (Aerts et al. 2003). And using the data of the Microvariability and Oscillation of Star (MOST) satellite, Walker et al. (2007) found that kappa1 Ceti has a differential rotation profile closely resembling that for the Sun. With ongoing and forthcoming space seismic missions: COvection, ROtatin and planetary Transits (COROT) (Baglin 2006) and Kepler (Christensen-Dalsgaard 2007), it is possible to extract the information on the internal rotation profile of solar-like stars.

Moreover, magnetic fields of the active regions on solar surface are believed to originate from strong toroidal magnetic fields generated by solar dynamo at the base of the convective zone. The understanding of both the stellar magnetic activity and the generation of magnetic fields is dependent on the information about the interior rotational properties of stars (Thompson et al. 2003; Fan 2004; Charbonneau 2005). However the evolution of rotation profile inside stars is poorly understood. Therefore it is an important problem to get a global picture of the evolution of rotation profile inside stars.

The influence of rotation on the stellar structure and evolution is studied by many investigators (Kippenhahn & Thomas 1970; Endal & Sofia 1976; Pinsonneault et al. 1989; Meynet & Maeder 1997; Huang et al. 2007). Redistribution of angular momentum within the interiors of stars has also been considered by many authors (Endal & Sofia 1981; Chaboyer et al. 1995; Maeder & Meynet 2000; Palacios et al. 2003; Huang 2004). These studies show that hydrodynamic angular momentum transport processes are unefficient in stars. Therefore magnetic angular momentum transport or other mechanisms should be considered in rotating stars. In addition, magnetic angular momentum transport in massive stars has been investigated by Maeder & Meynet (2003, 2004, 2005). The massive stars with magnetic fields rotate almost as a solid body throughout the whole star (Maeder & Meynet 2004). Eggenberger et al. (2005) and Yang & Bi (2006) study the rotation profile of the Sun and show that the quasi-solid rotation in the Sun can be achieved by considering the effect of the magnetic fields. In this paper, we mainly focus on the internal rotation profiles of solar-like stars. In Sect. 2 diffusion coefficient of magnetic angular momentum transport is given. In Sect. 3 numerical calculation and results are presented. Then, discussion and conclusion are made in Sect. 4.

2 DIFFUSION COEFFICIENT OF MAGNETIC ANGULAR MOMENTUM TRANSPORT

Spruit (1999; 2002) developed the Tayler-Spruit dynamo, which can generate magnetic fields in the radiative region of differentially rotating stars. These fields are predominantly azimuthal components, $B \sim B_\phi$. If magnetic fields exist in stars, magnetic angular momentum transport can be described by magnetic induction and momentum equations. For a constant magnetic diffusivity and stellar rotation (Zahn 1992), under axisymmetry and only considering Lorentz force, the azimuthal components of the induction and momentum equations are (Barnes et al. 1999; Yang & Bi 2006)

$$\frac{\partial B_\phi}{\partial t} + \eta \left(\frac{1}{r^2 \sin^2 \theta} - \nabla^2 \right) B_\phi = r \sin \theta \mathbf{B}_p \cdot \nabla \Omega, \quad (1)$$

$$\rho r^2 \sin^2 \theta \frac{\partial \Omega}{\partial t} = \frac{1}{4\pi} \mathbf{B}_p \cdot \nabla (r \sin \theta B_\phi). \quad (2)$$

If the effect of the magnetic diffusivity is to limit the growth of the toroidal field after some time, the growth of the instability is halted by dissipative processes that operate on a timescale τ . Accordingly the second term on the left-hand side of Eq. (1) may be replaced simply by B_ϕ/τ (Barnes et al. 1999). Substituting for the second term of Eq. (1) and differentiating the Eq. (1) with respect to time, one can obtain (Barnes et al. 1999)

$$\frac{\partial^2 B_\phi}{\partial t^2} + \frac{1}{\tau} \frac{\partial B_\phi}{\partial t} = r \sin \theta \mathbf{B}_p \cdot \nabla \frac{\partial \Omega}{\partial t}. \quad (3)$$

For much longer times than the timescale of the instability, one would expect the term involving the first time derivative to dominate (Barnes et al. 1999), so that

$$\frac{1}{\tau} \frac{\partial B_\phi}{\partial t} \approx r \sin \theta \mathbf{B}_p \cdot \nabla \frac{\partial \Omega}{\partial t}. \quad (4)$$

For shellular rotation $\Omega(r, \theta) \sim \Omega(r)$ (Zahn 1992), then

$$B_\phi \sim \tau r \sin \theta B_r \frac{\partial \Omega}{\partial r}. \quad (5)$$

Using Eq. (5), equation (2) can be rewritten as

$$\begin{aligned} \rho r^2 \frac{\partial \Omega}{\partial t} &\approx \frac{1}{4\pi \sin^2 \theta} \mathbf{B}_p \cdot \nabla (\tau r^2 \sin^2 \theta B_r \frac{\partial \Omega}{\partial r}) \\ &\approx \frac{B_r}{4\pi} \frac{\partial}{\partial r} (\tau r^2 B_r \frac{\partial \Omega}{\partial r}) \\ &\approx \frac{1}{r^2} \frac{\partial}{\partial r} (\frac{\tau B_r^2}{4\pi \rho} r^4 \rho \frac{\partial \Omega}{\partial r}). \end{aligned} \quad (6)$$

The diffusion coefficient for angular momentum transport can thus be obtained as

$$D_m = \frac{\tau B_r^2}{4\pi \rho}. \quad (7)$$

In paper I (Yang & Bi 2006) we also got a similar diffusion coefficient, but it was only an assumption that the coefficient can be used in the equation of the transport of angular momentum. From Eq. (6) it can be found that the magnetic angular momentum transport approximately obeys the diffusion coefficient D_m .

For a steady equilibrium, the dissipating timescale τ has to match the growth timescale σ^{-1} of the instability. Using the growth time scale of magnetic instability given by Pitts & Tayler (1985) and Spruit (1999),

$$\sigma^{-1} = \frac{\Omega}{\omega_A^2}, \omega_A = \frac{B_\phi}{(4\pi \rho)^{1/2} r}, \quad (8)$$

one can get the diffusion coefficient

$$\begin{aligned} D_m &= \frac{B_r^2}{4\pi \rho} \frac{\Omega}{\omega_A^2} \\ &= r^2 \Omega \left(\frac{B_r}{B_\phi} \right)^2. \end{aligned} \quad (9)$$

Equation (9) can also be rewritten as

$$D_m = r^2 \Omega \left(\frac{\omega_{rA}}{\omega_A} \right)^2, \quad (10)$$

where

$$\omega_{rA} = \frac{B_r}{(4\pi \rho)^{1/2} r}. \quad (11)$$

Equation (10) hints that magnetic angular momentum transport is related to Alfvén waves.

The distribution of magnetic fields inside a star is poorly known. One of the distributions of magnetic fields was given by Spruit (2002)

$$\frac{B_r}{B_\phi} = q \left(\frac{\Omega}{N_\mu} \right)^2, \quad (12)$$

where $q = -\frac{\partial \ln \Omega}{\partial \ln r}$, for the case 0 that the effect of thermal diffusion can be neglected, namely $N_\mu > N_T$, and

$$\frac{B_r}{B_\phi} = 2^{1/4} \left(\frac{\Omega}{N_T} \right)^{1/4} \left(\frac{\kappa}{r^2 N_T} \right)^{1/4} \quad (13)$$

for the case 1 with the effect of thermal diffusion. Using the expressions (12) and (13), one can rewrite Eq. (9) as

$$D_{m0} = r^2 \Omega q^2 \left(\frac{\Omega}{N_\mu} \right)^4 \quad (14)$$

for the case 0 and

$$D_{m1} = 2^{1/2} r^2 \Omega \left(\frac{\Omega}{N_T} \right)^{1/2} \left(\frac{\kappa}{r^2 N_T} \right)^{1/2} \quad (15)$$

for the case 1. Equations (14) and (15) are consistent with the effective magnetic viscosity defined by Spruit (2002) and Maeder & Meynet (2004) for the radial transport of angular momentum. The expression of (14) and (15) is only one of the cases of D_m . Braithwaite (2006) validates the Tayler-Spruit dynamo scenario, but which is contrary to the findings of Zahn et al. (2007). The rotation profile of massive stars with magnetic fields was investigated by Maeder & Meynet 2004. And the rotation profile of the Sun with magnetic fields was studied by Eggenberger et al. 2005. In this work we focus on solar-like stars with mass 1.0 - 1.5 M_\odot .

3 NUMERICAL CALCULATION AND RESULTS

3.1 Angular momentum transport and loss

The Yale Rotation Evolution Code (YREC7) is used to construct stellar models in its rotating configuration (Pinsonneault et al. 1989; Guenther et al. 1992). All models are evolved from fully convective pre-main sequence (PMS) to somewhere near the end of the Main Sequence (MS). The newest OPAL EOS-2005¹ (Rogers & Nayfonov 2002), OPAL opacity (Iglesias & Rogers 1996), and the Alexander & Ferguson (1994) opacity for low temperature are used. The models take into account diffusion of helium and metals, using the prescription of Thoul et al. (1994). The initial chemical composition of the models is fixed at $Z_0 = 0.02$, $X_0 = 0.706$.

Hydrodynamic instabilities considered in the YREC7 have been presented by Pinsonneault et al. (1989). It is assumed that convection enforces solid-body rotation in the convective regions of a star. Therefore the rotational instabilities are effective only in the radiative regions. The transport of angular momentum is treated as (Endal & Sofia 1978; Pinsonneault et al. 1989)

$$\rho r^2 \frac{\partial \Omega}{\partial t} = f_\Omega \frac{1}{r^2} \frac{\partial}{\partial r} (\rho r^4 D \frac{\partial \Omega}{\partial r}) \quad (16)$$

¹ <http://physci.llnl.gov/Research/OPAL/>

Table 1 Model parameters

model	mass	J_0^a	f_k	$f_{\Omega 1}^b$	$f_{\Omega 2}^c$
	M_{\odot}	$10^{50} \text{ g cm}^2 \text{ s}^{-1}$			
M1.0a	1.0	1.591	3.0	1.0	0
M1.0b	1.0	1.591	3.0	1.0	0.01
M1.2	1.2	1.9095	3.0	1.0	0.01
M1.4	1.4	1.534	1.0	1.0	0.01
M1.5	1.5	1.095	1.0	1.0	0.01

^a The initial angular momentum;

^b The value of f_{Ω} for the coefficient of hydrodynamic instabilities (Pinsonneault et al. 1989);

^c The value of f_{Ω} for D_m ; model M1.0a with only hydrodynamic instabilities.

in the radiative regions of a star, where f_{Ω} is an adjustable parameter introduced to represent some inherent uncertainties in the diffusion equation. In stars with $M \leq 1.5M_{\odot}$, angular momentum loss due to magnetic braking is treated as a parameterized formula (Kawaler 1988)

$$\frac{dJ}{dt} = f_K K_{\Omega} \left(\frac{R}{R_{\odot}}\right)^{1/2} \left(\frac{M}{M_{\odot}}\right)^{-1/2} \Omega^3 \quad (17)$$

to reproduce the Skumanich relationship (Skumanich 1972), where $K_{\Omega} \simeq 1.13 \times 10^{47} \text{ g cm}^2 \text{ s}$, f_K is an adjustable parameter. It is assumed that the magnetic braking has an effect on the whole convective envelope. In some case, a PMS star could be locked by the surrounding accretion disk. However the disk can extract angular momentum from the star as well as can supply angular momentum to the star (Stassun & Terndrup 2003). Moreover, it has been argued by Matt & Pudritz (2005a, 2005b) that the spin-down of PMS stars may not be due to a magnetic star-disk interaction, but may result from a magnetic stellar wind. Thus for simplicity, we do not consider the magnetic star-disk interaction.

The initial angular momentum of a star is still uncertain. Kawaler (1987) shows that the angular momentum J of stars more massive than $1.5 M_{\odot}$ is proportional to squared mass M^2 . But the mass-momentum relation of stars below $1.5 M_{\odot}$ is uncertain. As a first test, we take the initial angular momentum to be a free parameter. The adjustable parameters mentioned above are listed in Table 1.

3.2 Results of calculation

Figure 1 compares the evolution of the internal rotation profile of $1.0 M_{\odot}$ models with only hydrodynamic instabilities given by Pinsonneault et al. (1989) and with both the hydrodynamic instabilities and magnetic fields. Both models are evolved from PMS with initial angular momentum $J_0 = 1.591 \times 10^{50} \text{ g cm}^2 \text{ s}^{-1}$ to the age of 4.5 Gyr. During the PMS phase, although with angular momentum loss from the surface of models, the rotation rate rapidly increases due to quickly contracting. The internal rotation profile of model with magnetic fields has been different from that of model with only hydrodynamic instabilities when the models are near the zero-age main sequence (ZAMS). The model with only hydrodynamic instabilities has a fast rotation core. The rotation of model with magnetic fields is, however, almost uniform. During the early stage of the MS, the rotation of the model M1.0a is differential, but the model M1.0b is a quasi-solid body rotation. At the age of 4.5 Gyr, the surface rotation rates of two models are around $2.7 \times 10^{-6} \text{ rad/s}$. However, internal distribution of angular velocity is

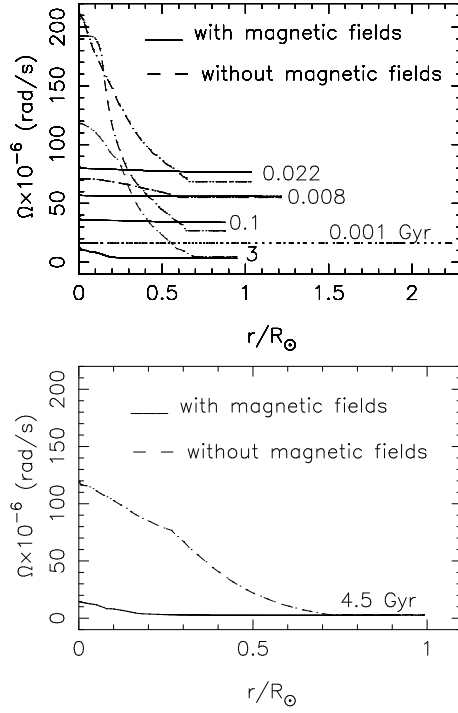


Fig. 1 Rotation profiles as a function of radius for $1.0 M_{\odot}$ model at different ages labeled by Gyr. The initial angular momentum $J_0 = 1.591 \times 10^{50} \text{ g cm}^2 \text{ s}^{-1}$. The dotted line indicates the solid-body rotation of the models with and without magnetic fields on the pre-main sequence.

quite different. The model M1.0a shows a strong differential rotation with a factor of about 40 between the angular velocity in the core and at the surface; but the model M1.0b shows an almost uniform angular velocity, with a small increase in $\Omega(r)$ in the center of $r < 0.2 R_{\odot}$, as that obtained by Eggenberger et al. (2005). The surface rotation rate of model M1.0b is higher than that of model M1.0a in the early evolutionary stage. And the loss rate of angular momentum is related to Ω^3 . Consequently the amount of the angular momentum loss of model M1.0b is larger than that of model M1.0a. The total angular momentum of model M1.0a is $2.628 \times 10^{49} \text{ g cm}^2 \text{ s}^{-1}$ at the age of 4.5 Gyr, which is about 13 times larger than the seismical result $(1.94 \pm 0.05) \times 10^{48} \text{ g cm}^2 \text{ s}^{-1}$ (Komm et al. 2003); but the total angular momentum of model M1.0b is $2.045 \times 10^{48} \text{ g cm}^2 \text{ s}^{-1}$ at the age of 4.5 Gyr, which is consistent with the result of helioseismology at the level of 3σ .

Figure 2 shows the evolution of the internal rotation profile of model M1.2. In the early evolutionary stage, the angular velocity $\Omega(r)$ is almost constant. At the stage of $X_c \sim 0.69$, about 90 percent of the initial angular momentum has been lost; the rotation is nearly uniform in the radiative region; but the rotation of the convective core is faster than that of the radiative region. There is a transition region between the convective core and the radiative region, where the angular velocity has a sharp radial change due to the spin-down of the outer parts of model resulting from angular momentum loss and the decrease of the horizontal

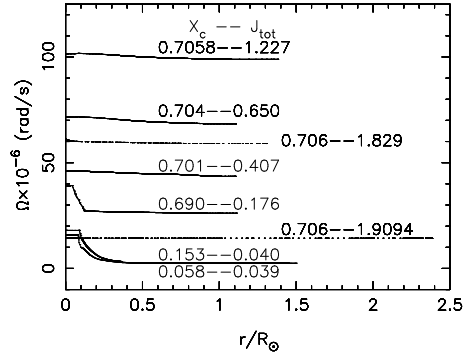


Fig. 2 Rotation profiles as a function of radius for model M1.2 at the different evolutionary stages indicated by the central hydrogen X_c . The initial angular momentum $J_0 = 1.9095 \times 10^{50} \text{ g cm}^2 \text{ s}^{-1}$. The J_{tot} is the total angular momentum of models in $10^{50} \text{ g cm}^2 \text{ s}^{-1}$. The lower dotted line shows the rotation profile of PMS model at the age of 1 Myr.

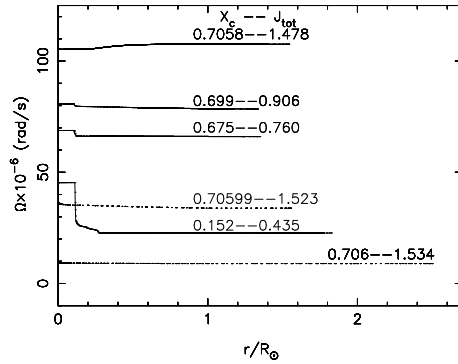


Fig. 3 Same as Fig. 2 but for model M1.4. The initial angular momentum $J_0 = 1.534 \times 10^{50} \text{ g cm}^2 \text{ s}^{-1}$.

coupling provided by the magnetic field resulting from the increase in μ -gradient in the region. The loss of angular momentum mainly occurs in the early evolutionary stage. During the late stage of the MS, the total angular momentum of model M1.2 is only several percent of the initial angular momentum; the rotation is slow; thus the loss rate of angular momentum is very low. Consequently, the angular momentum of model M1.2 is almost conservative from the stage of $X_c = 0.153$ to the stage of $X_c = 0.058$.

The evolution of the internal rotation profiles of models M1.4 and M1.5 are shown in Figs. 3 and 4. The model M1.4 has lost about 50 percent of the initial angular momentum at the stage of $X_c = 0.675$. But the model M1.5 has only lost about 15 percent of the initial angular momentum even at the stage of $X_c = 0.487$. The distributions of the angular velocity of models M1.4 and M1.5 are different from that of model M1.2. The angular velocity between the convective core and the radiative region of models M1.4 and M1.5 decreases obviously when the radius increases. The radial change of the angular velocity between the convective core and the radiative region in models M1.4 and M1.5 is larger than

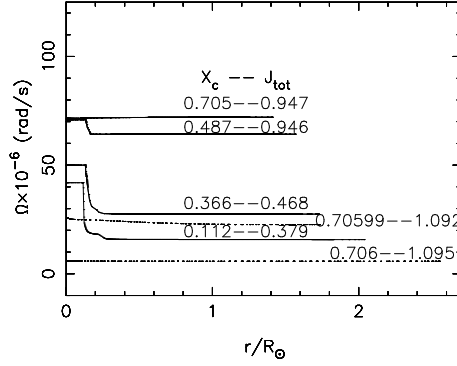


Fig. 4 Same as Fig. 2 but for model M1.5. The initial angular momentum $J_0 = 1.095 \times 10^{50} \text{ g cm}^2 \text{ s}^{-1}$.

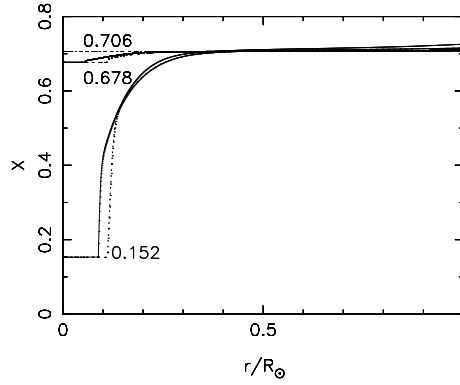


Fig. 5 Internal distribution of the hydrogen mass fraction X as a function of the radius. The solid lines show model M1.2. The dotted lines refer to model M1.4.

that in model M1.2, which should be due to the μ -gradient and the fast spin-down occurring at the same stage in models M1.4 and M1.5. However, in model M1.2, the fast spin-down occurs in the early evolutionary stage when the μ -gradient is small.

Figure 5 shows the distribution of the hydrogen mass fraction X of models M1.2 and M1.4. It is obvious that there is a sharp μ -gradient at the bottom of the radiative region of models M1.2 and M1.4 at the late stage of MS. The μ -gradient and the Ω -gradient are in the same region. The ratio of magnetic field, B_r/B_ϕ , is related to ∇_μ^{-1} in Tayler-Spruit dynamo, namely $D_m \sim \nabla_\mu^{-2}$. Thus the increase in μ -gradient must lead to the decrease in the coupling provided by magnetic fields. This scenario was first found by Eggenberger et al. (2005) in the Sun.

4 DISCUSSION AND CONCLUSIONS

The surface velocity is sensitive to the loss rate of the angular momentum. The equation (17) may overestimate the loss rate of angular momentum of the rapid rotation stars (Andronov et al. 2003). But it can reproduce the Sun's rotation.

Thus we take it in our models. The adjustable parameter, f_k , is adjusted to obtain the solar rotation rate at the age of 4.5 Gyr in models M1.0a and M1.0b. However the same value of f_k cannot be applied to models M1.4 and M1.5 because the convective envelope of models M1.4 and M1.5 is too shallow. Thus we take a small f_k for models M1.4 and M1.5.

The value of parameter $f_{\Omega 2}$ is adjusted to obtain a quasi-solid rotation in our models. The value of 0.01 can do work in our models. However this value is less than 1. This could be a consequence of overestimating the ratio of B_r to B_ϕ in Tayler-Spruit dynamo.

The distribution of angular velocity of models M1.0a and M1.0b shows that the rotation profile strongly depends on the efficiency of angular momentum transport. The angular momentum is effectively transported outward by magnetic fields in M1.0b. Thus the rotation of the core of M1.0b is slow comparing with that of M1.0a. The surface rotation rate mainly depends on the loss rate of angular momentum and the amount of outward transport of angular momentum. Because both M1.0a and M1.0b have same value of f_k and initial Ω , the discrepancy of the surface velocity between M1.0a and M1.0b relies on the efficiency of outward transport of angular momentum. In M1.0b, the loss of angular momentum is counteracted by magnetic angular momentum transport. Thus the surface velocity of M1.0b is higher than that of M1.0a when the interior of M1.0b has enough angular momentum to transport outward. The loss rate of angular momentum is related to Ω^3 . Consequently the amount of angular momentum loss of model M1.0b is larger than that of model M1.0a. This scenario takes place in the early evolutionary stage.

At the early stage of M1.2, the fast spin-down leads to the sharp radial change of angular velocity at the top of the convective core. But at the same stage of models M1.4 and M1.5, the spin-down is slow. At the late evolutionary stage of M1.2, although there is a large μ -gradient at the top of the core, the spin-down is very slow. Thus the radial change of the angular velocity is small comparing with that of models M1.4 and M1.5 at the top of the core. However in models M1.4 and M1.5, the μ -gradient and the fast spin-down resulting from angular momentum loss and stellar expansion occur on the same stage. Therefore the radial change of angular velocity is large at the top of the core in models M1.4 and M1.5.

The $1.0 M_\odot$ model with only hydrodynamic instabilities has a fast rotation core, and its total angular momentum is $2.628 \times 10^{49} \text{ g cm}^2 \text{ s}^{-1}$ at the age of 4.5 Gyr, which disagrees with the helioseismic results. However the $1.0 M_\odot$ model with magnetic fields has a slow rotation core, and the rotation is almost uniform in the radiative region, which are consistent with the seismic results. Moreover the total angular momentum of the model with magnetic fields is $2.045 \times 10^{48} \text{ g cm}^2 \text{ s}^{-1}$ at the age of 4.5 Gyr, which agrees with the helioseismic result at the level of 3σ .

A diffusion coefficient of magnetic angular momentum transport is obtained. Not only can the magnetic fields reproduce a quasi-solid rotation, but they can enhance the loss rate of angular momentum. The rotation of solar-like stars with magnetic fields is almost uniform in the radiative regions, which is consistent with the results of helio- and asteroseismology. However there is a transition region between the convective core and the radiative region, where the angular velocity has a sharp radial change, which is different from that of solar model and that of massive stars shown by Maeder & Meynet (2004). Moreover the changes of the angular velocity in the transition region increase with the increasing in the age and mass.

Acknowledgements This work was supported by the Ministry of Science and Technology of the People's republic of China through grant 2007CB815406, and by the NSFC through grants 10173021, 10433030, 10773003, and 10778601.

References

- Aerts C., Daszynska J., Scufflaire R. et al., 2003, *Sci*, 300, 1926
- Alexander D. R., Ferguson J. W., 1994, *ApJ*, 437, 846
- Andronov N., Pinsonneault M., Sills A., 2003, *ApJ*, 582, 358
- Baglin A., Michel E., Auvergne M. et al., 2006, In: K. Fletcher, M. Thompson, ed., *Proceeding of SOHO 18/GONG 2006/HELAS I, Beyond the spherical Sun*, ESA SP-624, p34
- Basu S., Christensen-Dalsgaard J., Thompson M. J., 2002, In: F. Favata, I. W. Roxburgh, D. Daladi-Enriquez, ed., *Proc. 1st Eddington Meeting 'Stellar Structure and habitable Planet Finding'*, ESA SP-485, 407
- Basu S., 2003, *Ap&SS*, 284, 153
- Barnes G., Charbonneau P., MacGregor K. B. 1999, *ApJ*, 511, 466
- Berthomieu G., Toutain T., Gonczi G. et al., 2001, In: A. Wilson, ed., *Proc. SOHO 10/GONG 2000 Workshop: Helio- and Asteroseismology at the Dawn of the Millennium*, ESA SP-464, 411
- Braithwaite J., 2006, *A&A*, 449, 451
- Chaboyer B., Demarque P., Pinsonneault M. H., 1995, *ApJ*, 441, 865
- Chaplin W. J., Christensen-dalsgaard J., Elsworth Y. et al., 1999, *MNRAS*, 308, 405
- Charbonneau P., 2005, *LRSP*, 2, 2
- Christensen-Dalsgaard J., Arentoft T., Brown T. M. et al., 2007, *CoAst*, 150, 350
- Eggenberger P., Maeder A., Meynet G., 2005, *A&A*, 440, L9
- Endal A. S., Sofia S., 1976, *ApJ*, 210, 184
- Endal A. S., Sofia S., 1978, *ApJ*, 220, 279
- Endal A. S., Sofia S., 1981, *ApJ*, 243, 625
- Fan Y., 2004, *LRSP*, 1, 1
- Gough D. O., Kosovichev A. G., 1993, *ASPC*, 40, 541
- Gough D. O., Kosovichev A. G., Toomre J. et al., 1996, *Sci*, 272, 1296
- Gough D. O., 1998, In: H. Kjeldsen, T.R. Bedding, eds., *The First MONS Workshop: Science with a Small Space Telescope*, Aarhus University: p. 33.
- Goupil M. J., Dziembowski W. A., Goode P. R. et al., 1996, *A&A*, 305, 487
- Guenther D. B., Demarque P., Kim Y. C. et al., 1992, *ApJ*, 387, 372G
- Huang R. Q., 2004, *A&A*, 422, 981H
- Huang R. Q., Song H. F., Bi S. L., 2007, *ChJAA*, 7, 235
- Iglesias C., Rogers F. J., 1996, *ApJ*, 464, 943
- Kawaler S. D., 1987, *PASP*, 99, 1322
- Kawaler S. D., 1988, *ApJ*, 333, 236
- Kippenhahn R., Thomas H. C., In *Stellar Rotation* (Slettebak, A., ed), New York: Gordon and Breach, 1970, p.20
- Komm R., Howe R., Durney B. R. et al., 2003, *ApJ*, 586, 650
- Lochard J., Samadi R., Goupil M. J., 2004, *SoPh.*, 220, 199
- Lochard J., Samadi R., Goupil M. J., 2005, *A&A*, 438, 939
- Maeder A., Meynet, G., 2000, *ARA&A*, 38, 43

- Maeder A., Meynet, G., 2003, *A&A*, 411, 543
Maeder A., Meynet, G., 2004, *A&A*, 422, 225
Maeder A., Meynet, G., 2005, *A&A*, 440, 104
Matt S., Pudritz R. E., 2005a, *MNRAS*, 356, 167
Matt S., Pudritz R. E., 2005b, *ApJ*, 632, L135
Meynet G., Maeder A. 1997, *A&A*, 321, 465
Palacios A., Talon S., Charbonnel, C. et al., 2003, *A&A*, 399, 603
Pinsonneault M. H., Kawaler S. D., Sofia S. et al., 1989, *ApJ*, 338, 424
Pitts E., Tayler R. J., 1985, *MNRAS*, 216, 139
Rogers F. J., Nayfonov A, *ApJ*, 2002, 576,1064
Roxburgh I. W., Audard N., Basu S. et al., 1998, In: J. Provost and F. X. Schmider, eds.,
Proc. IAU Symp. 181: Sounding Solar and Stellar Interiors, Nice Observatory, 245
Schou J., Antia H. M., Basu S. et al., 1998, *ApJ*, 505, 390
Skumanish A., 1972, *ApJ*, 171, 565
Spruit H. C., 1999, *A&A*, 349, 189
Spruit H. C., 2002, *A&A*, 381, 923
Stassun K. G., Terndrup D., 2003, *PASP*, 115, 505
Thoul A. A., Bahcall J. N., Loeb A., 1994, *ApJ*, 421, 828
Thompson M. J., Christensen-Dalsgaard J., Miesch M. S., et al., 2003, *ARA&A*, 41, 599
Walker G. A. H., Croll B., Kuschnig R. et al., 2007, *ApJ*, 659, 1611W
Yang W. M., Bi S. L., 2006, *A&A*, 449, 1161 (paper I)
Zahn J.-P., 1992, *A&A*, 265, 115
Zahn J.-P., Brun A. S., Mathis, S., 2007, *A&A*, 474, 145